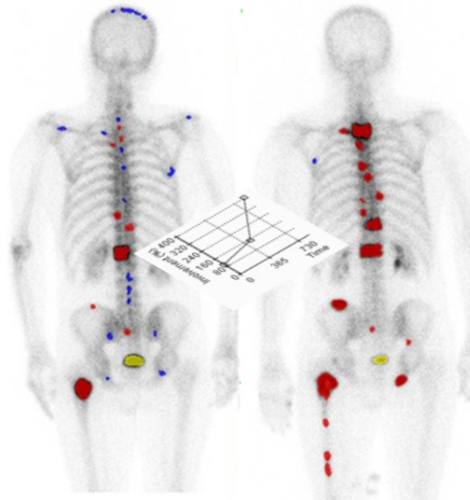


Quantitative Analysis of Bone Scans in Prostate Cancer Patients



Reza Kaboteh

Department of Molecular and Clinical Medicine
Institute of Medicine
Sahlgrenska Academy at University of Gothenburg



UNIVERSITY OF GOTHENBURG

Gothenburg 2013

Cover illustration: Reza Kaboteh

Quantitative Analysis of Bone Scans in Prostate Cancer Patients

© Reza Kaboteh 2013

reza.kaboteh@gu.se

ISBN 978-91-628-8757-5

Printed in Sweden by:

Ineko, Gothenburg 2013

Every great dream begins with a dreamer. Always remember, you have within you the strength, the patience, and the passion to reach for the stars to change the world.

Harriet Tubman

These studies were supported by:
University of Gothenburg, ALF grants and Region Västra Götaland FoU
grants.

Keywords: Image analysis – Radionuclide imaging – Bone metastases –
Prostate cancer – Automated detection – Computer assisted diagnosis –
Bone scan index

ISBN: 978-91-628-8757-5

Quantitative Analysis of Bone Scans in Prostate Cancer Patients

Reza Kaboteh

Department of Molecular and Clinical Medicine, Institute of Medicine
Sahlgrenska Academy at University of Gothenburg
Gothenburg, Sweden

ABSTRACT

Prostate cancer (PCa) is one of the most common diseases in the world. PCa can primarily disseminate to the bone, causing bone metastases, which in turn can lead to death. To treat the disease it is important to diagnose bone metastases as soon as possible. Bone metastases are diagnosed usually by bone scan imaging. However, interpretation of bone scan images is not always an easy task for physicians. One way of minimising the risk of misinterpretation is quantitative analysis of bone scan images in order to ascertain whether they show any metastatic lesions, and if so, to what extent. Quantification of the bone scan, i.e. the bone scan index (BSI) method, could be used for prognostication of survival, or to follow up the effect of treatment. The aim of the thesis was to develop and validate a fully automated method for the quantification of skeletal images in patients with prostate cancer based on the BSI method. This thesis is based on four papers. In paper 1, *"A Novel Automated Platform for Quantifying the Extent of Skeletal Tumour Involvement in Prostate Cancer Patients Using the Bone Scan Index"*, we developed an automated BSI-quantification method, used it in a training group of 795 patients, compared it to a manual method and assessed the prognostic value of BSI in an evaluating group of 384 patients. The automated method showed a good correlation ($r=80\%$) with the manual method, and BSI was strongly associated with prostate cancer death. In paper 2, *"Bone Scan Index: a prognostic imaging biomarker for high-risk prostate cancer patients receiving primary hormonal therapy"*, we found that BSI included prognostic information in addition to other clinical parameters such as "prostate-specific antigens". Patients with $BSI < 1$ had a much higher survival rate after 5 years than those with $BSI > 5$. In paper 3, *"Progression of Bone Metastases in Patients with Prostate Cancer - Automated Detection of New Lesions and Calculation of Bone Scan Index"*, we further develop the automatic method to find new metastases using a training group of 266 patients. The method evaluated 31 patients who received chemotherapy. Patients with an increase in BSI during treatment had a lower two-year survival rate (18%) than those with a decrease in BSI (57%). In the final paper, *"Assessment of baseline and longitudinal bone scan index measures in the context of a randomised placebo-controlled trial of tasquinimod in men with metastatic castration-resistant prostate cancer (mCRPC)"*, we retrospectively calculated BSI at baseline and upon treatment in 85 patients from a clinical trial. We found that BSI and BSI change on-treatment were associated with survival. BSI correlated with known biomarkers of survival, but adds independent prognostic information. In conclusion, BSI calculated using an automated method contains prognostic information and can be used to evaluate treatment effects.

POPULÄRVETENSKAPLIG SAMMANFATTNING

Prostatacancer (PCa) är den vanligaste cancer sjukdomen. PCa kan sprida sig till andra organ, framförallt till skelettet och orsaka skelettmetastaser (Sm). Skelettscintigrafi är den vanligaste metoden för att undersöka om en patient har Sm eller inte. Patienter med mycket utbredda Sm har sämre överlevnad men det finns ingen kliniskt användbar metod att beskriva detta. En sådan kvantifiering skulle kunna användas för att bedöma PCa patienternas överlevnad eller om en behandling är effektiv eller inte.

Syftet med avhandlingsarbetet var att utveckla och testa en helt automatisk metod för kvantifiering av skelettbilder från patienter med PCa. Metoden baseras på en tidigare beskriven manuell metod som kallas Bone Scan Index (BSI). Arbetet beskrivs i fyra sammanhängande studier.

I första studien, *“A Novel Automated Platform for Quantifying the Extent of Skeletal Tumour Involvement in Prostate Cancer Patients Using the Bone Scan Index”*, utvecklade vi en helt automatisk metod baserad på nya bildbehandlingslösningar, artificiella neurala nätverk och en träningsgrupp som bestod av 795 skelettbilder. Metoden testades på 384 PCa patienter som undersökts med skelettscintigrafi i samband med att de fick sin diagnos. Resultaten visade att de med ett BSI-värde mindre än 1 hade en bättre överlevnad än de med högre värden.

I arbete 2, *“Bone Scan Index: a prognostic imaging biomarker for high-risk prostate cancer patients receiving primary hormonal therapy”*, visade vi att BSI metoden innehöll prognostisk information i tillägg till den som cancertyp, spridning och blodprover, speciellt prostata specifik antigen (PSA), innehåller. 5-årsöverlevnaden var betydligt bättre hos patienter med låga BSI än hos de med höga BSI värde.

I tredje arbetet, *“Progression of Bone Metastases in Patients with Prostate Cancer – Automated Detection of New Lesions and Calculation of Bone Scan Index”*, vidareutvecklade vi BSI metoden för att hitta nya Sm när två skelettbilder från samma patient studerades. Nya Sm under behandling är ett tecken på att behandlingen inte är effektiv. Vi testade metoden på 31 patienter som undersökts före och under kemoterapi. De som fick en ökning i BSI under behandlingen hade sämre överlevnad än de där BSI minskade.

I sista arbetet, *“Assessment of baseline and longitudinal bone scan index measures in the context of a randomized placebo-controlled trial of*

tasquinimod in men with metastatic castration-resistant prostate cancer (mCRPC)”, testade vi BSI i en grupp av 85 patienter som ingått i en läkemedelsstudie och som undersökts med skelettscintigrafi före och 12 veckor efter behandlingsstart. BSI-värdet före behandling och förändring av BSI under behandlingen hade ett direkt samband med överlevnad. Ju högre BSI värde eller ökning av BSI desto lägre överlevnad.

Sammanfattning: Kvantifiering av skelettscintigrafiska bilder har ett prognostiskt värde och det kan användas för att utvärdera behandlingseffekt hos PCa patienter.

LIST OF PAPERS

This thesis is based on the following studies, referred to in the text by their Roman numerals.

- I. Ulmert D*, Kaboteh R*, Fox J , Savage C, Evans M , Lilja H, Abrahamsson P-A, Björk T, Gerdtsson A, Bjartell A, Gjertsson P, Höglund P, Lomsky M, Ohlsson M, Richter J, Sadik M, Morris M , Scher H , Sjöstrand K, Yu A, Suurkula M, Edenbrandt L, Larson S M. A Novel Automated Platform for Quantifying the Extent of Skeletal Tumour Involvement in Prostate Cancer Patients Using the Bone Scan Index.
Eur Urol 2012, 62:78
- II. Kaboteh, R, Damber J-E, Gjertsson P, Höglund P, Lomsky M, Ohlsson M, Edenbrandt L. Bone Scan Index: a prognostic imaging biomarker for high-risk prostate cancer patients receiving primary hormonal therapy.
EJNMMI Res 2013, 3:9
- III. Kaboteh R, Gjertsson P, Leek H, Lomsky M, Ohlsson M, Sjöstrand K, Edenbrandt L. Progression of Bone Metastases in Patients with Prostate Cancer – Automated Detection of New Lesions and Calculation of Bone Scan Index.
EJNMMI Res 2013, 3:64
- IV. Armstrong A.J*, Kaboteh R*, Carducci M.A, Damber J-E, Stadler W.M., Hansen M, Edenbrandt L, Forsberg G, Nordle Ö, Pili R, Morris M. Assessment of baseline and longitudinal bone scan index measures in the context of a randomized placebo-controlled trial of tasquinimod in the men with metastatic castration-resistant prostate cancer (mCRPC).
Manuscript

* Equal contribution

CONTENT

ABBREVIATIONS.....	4
1 INTRODUCTION.....	8
1.1 Prostate cancer.....	8
1.2 Risk factors.....	9
1.3 Diagnose of prostate cancer.....	11
1.4 Treatment of prostate cancer.....	14
1.5 Imaging.....	15
1.5.1 Bone scan.....	15
1.5.2 SPECT/CT.....	18
1.5.3 MRI.....	18
1.5.4 PET.....	18
2 AIM.....	20
3 METHODS.....	21
3.1 Quantification of images.....	21
3.2 Segmentation.....	22
3.3 Normalization and hotspots detection.....	26
3.4 Hotspots quantification.....	27
3.5 Hotspot classification.....	28
3.6 Bone scan index.....	29
3.7 Bone scan examination.....	30
4 PATIENTS.....	32
4.1 Study design.....	32

4.2	
Population.....	32
5 STATISTICAL ANALYSIS.....	34
6 RESULTS.....	35
6.1 Automated vs. manual method.....	35
6.2 BSI as a prognostic tool.....	36
6.3 BSI as treatment-response tool.....	37
7 DISCUSSION.....	38
8 CONCLUSION.....	41
9 DISCLOSURE.....	42
ACKNOWLEDGEMENT.....	43
REFERENCES	46
ORIGINAL PAPERS.....	52

ABBREVIATIONS

AJCC	American Joint Committee on Cancer
ANN	Artificial Neural Network
Blca	Bladder cancer
Bra	Breast cancer
BSI	Bone scan index
CAD	Computer assisted diagnosis/ Computer assisted detection
CI	Confidence interval
C-index	Concordance index
CRP	C-reactive protein
CRPC	Castration-resistant prostate cancer
CT	Computer tomography
DRE	Digital rectal examination
EBRT	External beam radiation therapy
ERSPC	European randomized study screening for prostate cancer
Fig	Figure
HR	Hazard ratio
IQR	Interquartile range
IV	intravenous
Kica	Kidney cancer
LDH	Lactate dehydrogenase

MBq	Megabecquerel
MCDS	Malmö Diet and Cancer Study
mCRPC	metastatic castration-resistant prostate cancer
MDP	Methylene diphosphonate
MPP	Malmö Preventive Medicine Project
MRI	Magnetic resonance imaging
MSKCC	Memorial Sloan-Kettering Cancer Center
NPCR	National Prostate Cancer Registry
OS	Overall survival
P	Placebo
PCa	Prostate cancer
PCWG2	Prostate cancer working group 2
PET	Positron emission tomography
PFS	Progression free survival
PSA	prostate-specific antigen
RR	Relative risk
SD	Standard deviation
Sm	Skelettmastaser
SE	Standard error
SPECT	Single photon emission computer tomography
T	Tasquinimod
TASQ	Tasquinimod

TRUS	Transrectal ultrasound
USA	United States of America
VAS	Visual analog scale
vs	Versus

1 INTRODUCTION

1.1 Prostate cancer

Prostate cancer (PCa) is one of the most frequent diseases in the world and the most common male cancer in Sweden. The incidence of prostate cancer varies widely across the globe. The incidence is higher in developed countries like the United States, Australia, New Zealand, Sweden and the United Kingdom. In the developing countries, on the other hand, we have a much lower incidence, according to data from the International Agency for Research on Cancers, reported in 2008 (1). The frequency of new cases in the United States is about 250,000 per year, with a mortality rate of 25% (2). The situation is the same in the United Kingdom (40,000 new cases and a 25% mortality rate) as in Sweden (9,663 newly diagnosed cases in 2011 and a 25% mortality rate). In Sweden the incidence rate has tripled since 1970 (Fig. 1). In 2010 PCa was the leading cancer incidence (33%) in our country, with a 2.4 per cent growth per year according to the National Board's report of 2011 (2). Prostate-specific antigen (PSA) screening is the most important reason for the high detection rate of PCa, though the incidence rate of PCa detection has decreased slightly over the last few years, and we do not know how the trend will evolve in the future (3).

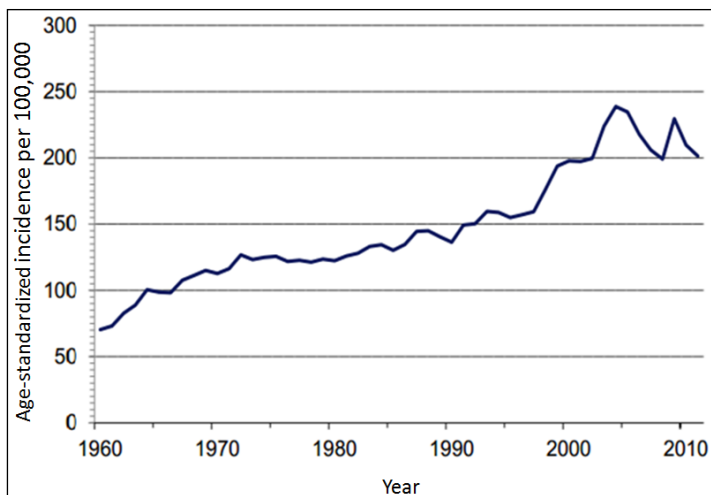


Figure 1. Incidence of prostate cancer in Sweden, 1960-2010.

1.2 Risk factors

Several risk factors correlate with PCa, even if the underlying reason for PCa remains obscure.

Age

One of the major risk factors for PCa is ageing. A PCa diagnosis is very unlikely in anyone under the age of 50. The highest incidence rate is around 65 to 80 years (Fig. 2) (2, 4), though PCa is more curable in younger patients than in older ones, according to Carter et al (5). If a curative treatment is to be started, a certain duration of expected survival is usually required. Curative treatment is thus recommended as being preferable for younger patients. The reason for the exponential increase in the prevalence of prostate cancer by ageing remains unknown (6).

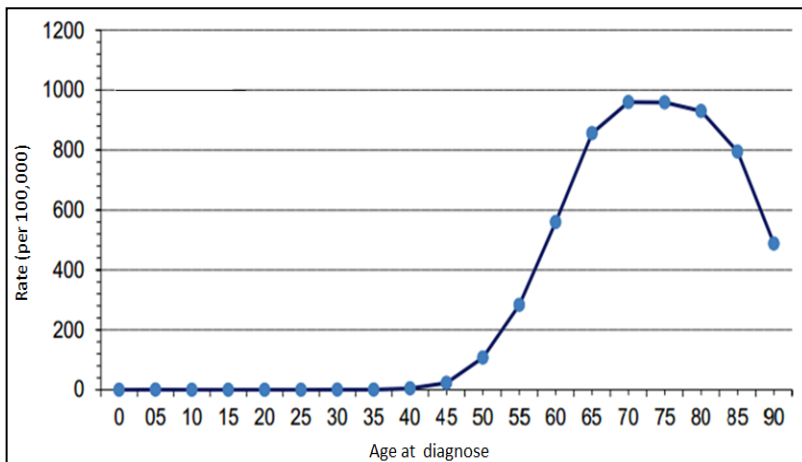


Figure 2. Incidence of prostate cancer and age. Cancer Statistics National Board.

The prevalence and mortality of PCa is multiplied by ageing. In fact, we cannot find any other disease in which prevalence and mortality increase as fast as they do in prostate cancer (6). The results of autopsy studies of men aged over 50 from several countries show an average of 22% as having latent prostate cancer. More than 70% of all patients with latent prostate cancer in the United States are over the age of 65. On the other hand, the probability of

getting PCa is less than 0.006% in men younger than 39, while this risk rises to over 2% around the age of 50 (7).

Heredity

Another risk factor for prostate cancer is heredity. Patients with relatives with a history of PCa were at greater risk of being diagnosed with PCa. In a review, Bratt et al pointed out a strong relationship between PCa and hereditary factors (8, 9). Genetic factors are deemed to be powerful determinants of prostate cancer.

Ethnicity

In the US prostate cancer is more common amongst African Americans, in whom the mortality rate is higher than in Caucasians. Makridakis et al showed an association of mis-sense substitution in SRD5A2 gene between genetic factor in African Americans and a higher incidence of PCa than in other groups (10).

Diet

Among the risk factors of PCa diet has been mentioned. One clear difference between the U.S. and Western Europe on the one hand and Asian countries like Japan and China on the other hand is lifestyle and eating habits. Chinese and Japanese people eat a lot more vegetables and seafood than we eat in the western world. Sofi et al has been previously presented a study confirming the health benefits of the Mediterranean diet in cardiovascular disease and even a reduced mortality from cancer (11). Men with a high consumption of meat, cheese, eggs, and milk have a relatively higher risk of fatal PCa than others (12).

Obesity

A public health problem in the Western world and particularly in the U.S. is obesity, which is a known determinant of cardiovascular disease and diabetes, but has also proved to be a risk factor for death from PCa. Several studies have identified a direct correlation between obesity and the risk of dying from the aggressive type of PCa. In a study of 800 patients from the U.S. it was found that those with a body mass index over 25 were at 1.6 times greater risk of dying from their disease (13).

Smoking

Smoking has been suggested as a risk factor for PCa. A large study in California including more than 43,000 men showed an increase of at least 1.9 in the relative risk (RR) in men smoking one pack of cigarettes per day (14, 15).

1.3 Diagnosis of prostate cancer

As PCa is a major health concern in the western world, it is crucial to detect any abnormality in time to decide whether an appropriate treatment option is necessary. An increased level of serum PSA over 4 ng/ml value in elderly men is the first sign of malignancy in the prostate gland. Younger adults should not have a PSA value of more than 2-3ng/ml (Fig. 3) (16).

PSA screening of asymptomatic healthy men is one of the most controversial issues in medical debates. PSA is a protein specific to the prostate and it has been shown to be a very effective method of detecting early forms of PCa. PSA has been available since the late 1980s and quickly became very popular in the U.S. leading to a highly increasing incidence of PCa in the early 1990s (17).

It is noticeable that an elevated PSA value does not necessary imply that the patient has PCa, as the PSA value increases with age, as it can be seen in 25% of patients with benign prostate hyperplasia (18) or in men with acute bacterial prostatitis (17). Besides PSA testing in order to detect many cases of PCa, a statistical model has been proposed in order to find indolent type of PCa (19).

At first glance, PSA testing appears to be an ideal health test. It is a low cost method, easy to obtain, and easy to interpret. Moreover, PCa found as a result of PSA testing is often curable. When the disease is detected as a result of clinical symptoms, it is almost not always possible to cure (19). 11-year follow-up results from the European Randomized Study of Screening for Prostate Cancer (ERSPC) showed a 29% relative reduction in the risk of death from PCa. This result is not in agreement with the US-based study by which 44% of participant underwent a PSA screening. The latter study did not show a significant difference in mortality caused by PCa, i.e. no benefit from PSA screening (20). Even if there is a decrease in PCa-caused mortality according to the ERSPC study, we still need to screen 1,000 people to find 20

PCa patients who need to be treated in order to save one life (21). Hugosson et al presented the result of 14-year follow-up screening of PCa by a 44% reduction in mortality from PCa, however; this reduction in mortality needed screening of 239 men to treat 12 in order to save one life. Side effects and overtreatment are considerable issues that make the benefits of PSA screening doubtful (22). Another aspect is that many patients are elderly men who probably die from some cause other than PCa, because the PCa is a low growing disease and often without any symptoms. The challenge is to find those patients who may derive benefit from treatment and suffer from an aggressive type of PCa. If this is a reasonable argument in this issue, the risk stratification will be the first step towards managing a treatment strategy. Neither Sweden nor the United States or other national health authorities currently recommend screening for PCa with PSA tests.

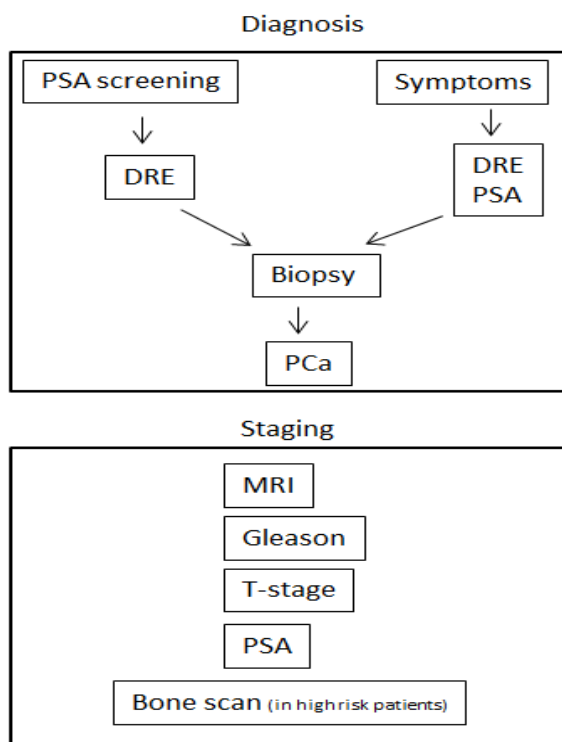


Figure 3. Illustration of different steps in diagnosis and staging of prostate cancer. DRE=Digital rectal examination, PSA= Prostate-specific antigen, MRI=Magnetic resonance imaging.

A digital rectal examination (DRE) is carried out so as to identify pathological changes in patients with symptoms or with high PSA levels from a screening examination. A histopathological verification is performed in order to confirm malignancy of the prostate. The European guideline for confirmation of suspected PCa recommends a transrectal ultrasound (TRUS)-directed repetitive biopsy. Further, it will be needed to identify whether the PCa abnormality is localized or whether the cancer cells have disseminated to adjacent organ. Magnetic resonance imaging (MRI) is recommended for local staging of PCa (16).

One of the most important factors in PCa staging is to determine whether it has spread to other organs. The most commonly used staging system for categorisation of cancer is the system proposed by American Joint Committee on Cancer (AJCC) called the TNM-staging system (23).

“T” describes the size of the primary tumour and whether it has disseminated to adjacent tissue.

“N” describes the presence of cancer cells in the adjacent lymph nodes.

“M” stands for metastasis, i.e. dissemination of cancer to distant organs.

Clinical T stage is used in combination with a Gleason score and PSA values to stratify patients with localized PCa into low-risk, intermediate-risk or high-risk categories (Table 1) (24)

	Gleason score		Clinical stage		PSA
Low risk	≤ 6	+	T1c-T2a	+	≤ 10 ng/ml
Intermediate risk	7	or	T2b-T2c	or	$>10-20$ ng/ml
High risk	8-10	or	T3-T4	or	>20 ng/ml

Table 1. Risk stratification of clinically localized prostate cancer patients

1.4 Treatment of prostate cancer

Patients with PCa in different stages of the disease are given different types of treatment (Fig. 4). Active surveillance or watchful waiting is a common alternative in asymptomatic PCa patients with localized disease and low-risk based on T-stage, Gleason score and PSA. Radical prostatectomy with or without external-beam radiation therapy (EBRT), or interstitial implantation of radioactive isotopes (25, 26) is more common in high risk patients. In more advanced stages of localized PCa, hormonal therapy such as orchiectomy or luteinizing hormone-releasing hormone (LH-RH) agonist is also common in combination with EBRT.

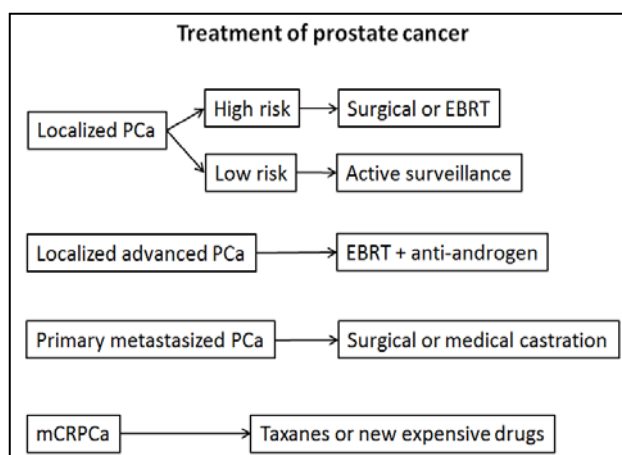


Figure 4. Treatment option for different stages of prostate cancer (localized, localized advanced, primary metastasised and metastatic castration-resistant) based on severity of PCa.

At a more advanced stage of the disease, metastatic castration-resistant prostate cancer (mCRPC) bone metastases are present and hormonal treatment is no longer efficient. PCa at this stage is not curable (25) and the treatment options have been bisphosphonate and anti-mitotic chemotherapy (Docetaxel) (27). With treatment, these patients experience pain relief, a decline in serum PSA and regression of metastases in soft tissue (27). Overall survival of these patients ten years ago was not more than 16 months, but with treatment survival has improved to up to 3 years (28).

Recently, new alternative treatments to chemotherapy with lower side effects have been developed (29). They directly target the cancer cells angiogenesis or have anti-metastatic mechanisms. Abiraterone (30) and MDV3100 are already approved and Tasquinimod (26), Orteronel (TAK700) (31) have been shown to be effective with few adverse events in recent phase I/II and III studies.

Ageing of the population i.e. the increasing proportion of elderly people in the population is due to several factors for example, economic, social and medical progress in the western world. This will result in more elderly men who consequently suffer from age-related diseases of which PCa is one of the most significant. This will result in a rapid increase in medical health care costs in the community (32). One way to approach this challenge is how to utilize the available health care resources optimally. How can we find the PCa patients who may derive benefit from expensive cancer drugs?

In 1996 Sweden's National Prostate Cancer Registry (NPCR) began registering all patients diagnosed with PCa. Information about the disease, changes in tumour characteristics and treatment in different geographical regions is actively monitored. This type of information can be used in the search for adequate treatment strategies for future patients.

1.5 Imaging

Accurate staging is important in the management of PCa patients. Low risk patients, based on Gleason score, Clinical T stage and PSA values, have a low probability for metastatic disease, and imaging is not recommended. In high risk patients, different imaging options are possible (33).

1.5.1 Bone scan

The most widely used imaging modality for detection of pathological changes in bone – osteoblastic activity – is bone scintigraphy. The main clinical indication for bone-scan imaging is evaluation of metastatic disease. The most common patient group referred for bone scans is prostate-cancer patients who are being examined to diagnose metastatic disease. Referrals are especially common in high-risk patients and for evaluation of treatment response. Prostate cancer has a tendency to disseminate to lymph nodes and the skeleton as the preferred organs (34).

This non-invasive nuclear-medicine imaging examination is performed using a gamma camera (Fig. 5). Whole-body bone scans are obtained three to four hours after administration of 600 MBq ^{99m}Tc -methylene diphosphonate (MDP) (35). The scanning procedure takes about 25 minutes and the result is two two-dimensional images – an anterior and a posterior image. These two-dimensional images are usually enough to show whether there are any pathological changes in the skeleton.



Figure 5. A gamma camera with capability to acquire planar whole-body and tomography images.

The MDP uptake process is believed to occur mainly through crystallisation of hydroxyapatite and partly through formation of calcium phosphate, resulting in bone mineralisation. The MDP uptake in the skeleton is proportional to osteoblastic activity, e.g. bone repair, which in turn leads to an increased blood supply to the bone (36). Half of the injected radioactive tracer accumulates in the bone, with the highest concentration being attained after one hour. The greater part of the tracer will have left the vascular bed three hours after injection, and image quality is normally optimal at this time, with activity in the soft tissue being low in relation to that in the skeleton. Bone scanning is a sensitive method, and abnormal uptake in a bone scan, i.e. increased osteoblastic activity, can be detected before increased density can be detected using radiological modalities (37).

MDP undergoes glomerular filtration, and distribution is thus dependent on renal function (37). In patients with normal renal function there will only be a few per cent of MDP remaining in the soft tissue after three hours. In patients with decreased renal clearance, however, much higher levels can be seen (38).

Interpretation of a whole-body bone scan is a visual assessment, and is highly dependent on the level of experience of the nuclear-medicine physician (39). Areas with high tracer uptake in bone can be normal variants, but focal uptake in bone should always be considered carefully. High uptake could be caused by trauma, thus the patient history is important. Bone-scan readers should take into account the localisation, symmetry, shape and intensity of each lesion in order to distinguish pathological changes due to metastatic activity from degenerative changes in the skeleton. A normal and a pathological bone scan are illustrated in Fig. 6.

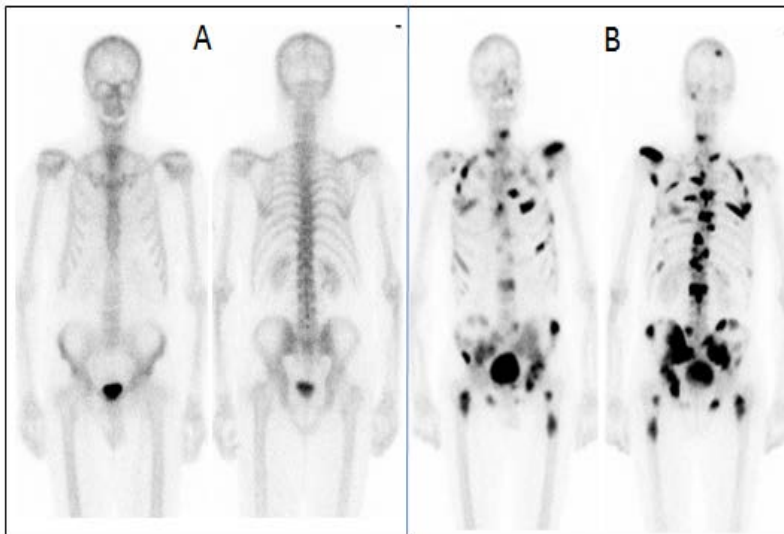


Figure 6. Normal (A) and pathological (B) bone scans (anterior and posterior projections).

1.5.2 SPECT/CT

Functional and structural information about cancer of different organs can be obtained using dual-modality imaging, e.g. computed tomography (CT) combined with single-photon-emission computed tomography (SPECT). The former provides the structural information on the body and the SPECT provides the functional data. The three-dimensional SPECT and CT images can be merged or shown in the same image, so that simultaneous analysis is possible (40). A SPECT/CT examination of the lower back can provide more precise information about the localisation of a lesion in a vertebra. The CT can also show whether there are any degenerative changes in the joints that could explain an increased tracer uptake in a bone scan.

1.5.3 MRI

Another imaging modality used in PCa patients is magnetic resonance imaging (MRI). This modality can be used for local staging of early prostate cancer (33, 41). With MRI it is possible to distinguish between soft tissues with different properties. A tumour in the prostate can be more accurately described in terms of location and in relation to other organs, especially with regard to the presence of extracapsular extension, but the use of MRI in PCa is still limited.

1.5.4 PET

Positron emission tomography (PET) is another nuclear-imaging modality, and it can provide high-resolution three-dimensional images of the human body. Intravenous injection of a positron-emitting radioactive tracer results in the emission of pairs of gamma rays, which the PET camera uses to build a three-dimensional image. This method, together with CT, has proven to be a successful imaging modality that offers much higher image resolution and greater specificity, enabling diagnosis of metastases in the bone and tumours in soft tissues (fig. 7). In high-risk prostate-cancer patients Sapir et al demonstrated greater sensitivity and specificity in the detection of bone metastases using ^{18}F -Fluoride PET/CT than using a planar whole-body bone scan (42). However, the limitation of PET and MRI scanning is that they are not available in many of the world's healthcare centres, and the cost of these imaging modalities is much higher than that of a bone scan.

A new hybrid imaging modality is PET/MRI. It is still mainly a research tool, but it may become important for the detection of malignancies in oncological imaging (43). PET/MRI could play a key cancer-management role in the field of molecular imaging, by means of which the pathway of tumour angiogenesis and the mechanism of the cell signalling system can be explained (44).

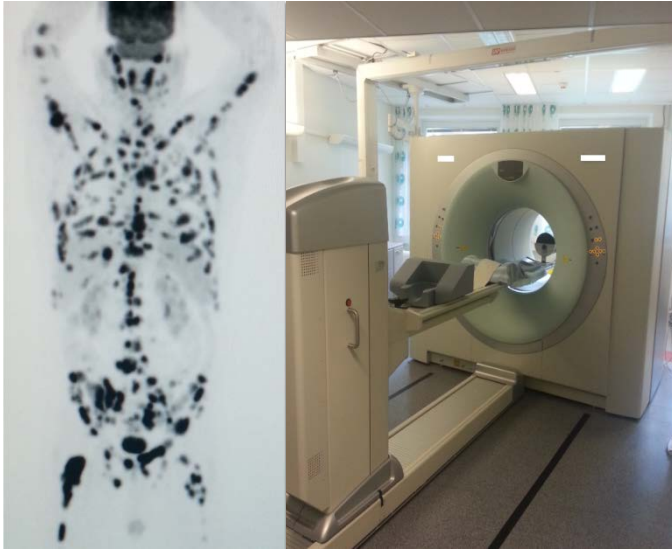


Figure 7. A PET/CT system for detection of metastatic disease and evaluation of treatment response in human body. Image to the left demonstrate a FDG-PET scan of a patient with widespread metastatic bone lesions.

2 AIM

The overall aim of this thesis was to develop and evaluate a new automated quantification method for analysis of bone scans in prostate-cancer patients. The specific purposes of these studies were as follows:

1. To develop a fully automated method for quantifying the percentage of the skeleton affected by tumour mass on a bone scan, based on the clinically validated methodology for manually computing the Bone Scan Index (BSI), and to determine the clinical value of automated BSI measurements beyond conventional clinical and pathologic features.
2. To explore the prognostic value of BSI obtained at the time of diagnosis in a group of high-risk prostate-cancer patients receiving primary hormonal therapy.
3. To develop and evaluate an automated method for the detection of new lesions and changes in BSI in serial bone scans, and to evaluate the prognostic value of the method in a group of patients receiving chemotherapy.
4. To evaluate the relationship between baseline BSI, other prognostic biomarkers and survival in the context of a randomised placebo-controlled trial of tasquinimod in men with metastatic castration-resistant prostate cancer (mCRPC).

3 METHODS

3.1 Quantification of Images

Over the last 30 years we have seen revolutionary developments in the field of medical imaging. Three-dimensional motion algorithms for calculation of myocardial elasticity using MRI (45), quantitative measurements of myocardial perfusion using PET (46) and quantification of left-ventricular function from gated SPECT (47) are a few examples. The internal organs, spine and brain can be visualised using three-dimensional volumetric imaging modalities such as MRI and CT. Quantitative measurements of breast density in mammography have proved to be a moderate risk factor for breast cancer (48, 49). Physicians in the field of nuclear medicine, however, usually base their reports on visual analysis of the images. Quantitative analysis is common in some areas in which cardiac function and perfusion are assessed, e.g. nuclear cardiology (50, 51). This type of information has proved to contain important diagnostic and prognostic data (52, 53), thus quantitative results are routinely included in cardiac reports. Quantitative analysis will probably also become more widely used in other areas, e.g. cancer imaging. Sullivan recently argued that radiologists should also provide quantitative data (54).

A quantitative method of bone-metastasis analysis was presented by a group at the Memorial Sloan-Kettering Cancer Center (MSKCC) (55). Their method was based on the proportional weights of each bone from the reference male (56), and the extent of skeletal tumour involvement in whole-body bone scans was presented as a Bone Scan Index (BSI). They later showed that the BSI was associated with survival in patients with prostate cancer (57). Their method of quantifying the extent of disease in whole-body bone scans has not, however, become widely used, one important reason for this probably being that its application is too time-consuming. The method was semi-automated, requiring the physician to mark bone structures containing lesions, after which a computer algorithm carried out the calculations of skeletal involvement.

Our recent experience in developing an automated computer-assisted diagnosis (CAD) system for the diagnosis of metastatic disease in whole-body bone scans formed the basis for the development of an automated BSI method (58). A diagram illustrating the different stages of the quantification

method is presented in Fig. 8. The methods have been incorporated into a commercially available software package developed by EXINI diagnostics AB (Lund, Sweden; <http://www.exini.com>).

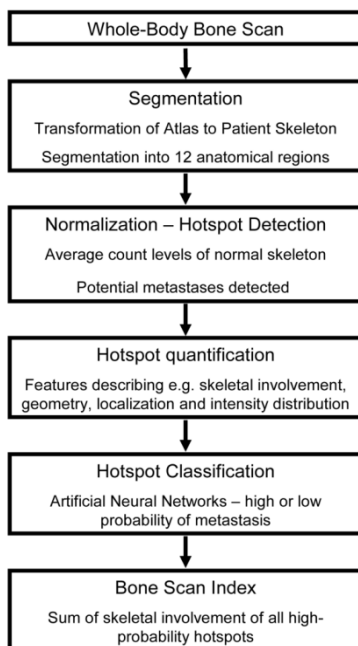


Figure 8. Illustration of steps of the quantification method

3.2 Segmentation

The entire skeleton, except for the distal parts of the arms and legs, is delineated automatically in both the anterior and posterior view. The distal extremities are not delineated, since they are often not acquired completely in routine bone scanning. The delineation is carried out by automatically fitting to the skeleton a manually delineated template known as an atlas, comprising one anterior and one posterior image (Fig. 9).

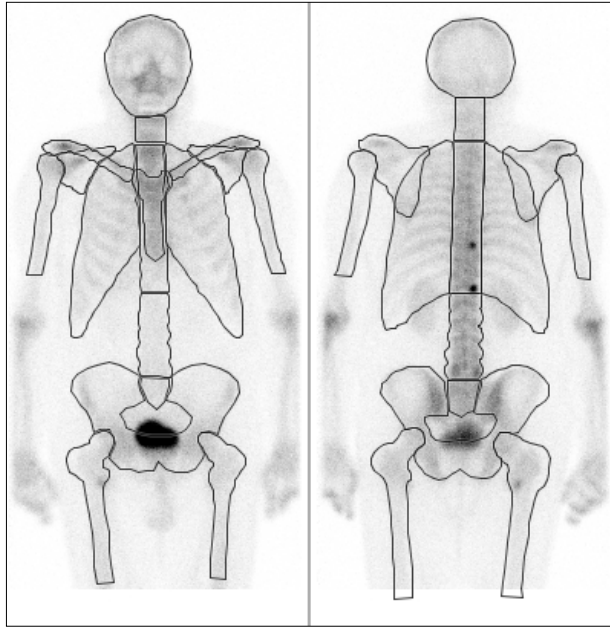


Figure 9. Segmentation of whole-body bone scans (anterior, left, and posterior, right, images) by automated method resulting in 12 anatomical regions

The fitting procedure is described in some detail below. The atlas is based on ten normal whole-body bone scans (five male and five female patients) from the training group (Fig. 10). The atlas was based on what Guimond and colleagues presented (59), and firstly involved fitting each of the ten normal scans to an arbitrarily selected member of the group of normal scans. The resulting ten image transformations are averaged to yield a transformation to a fictitious normal subject, with the average anatomy and intensity displayed by the normal group. In order to avoid any bias resulting from selection of a particular normal scan as a reference, the procedure is repeated once using the newly acquired fictitious normal scan as a reference.

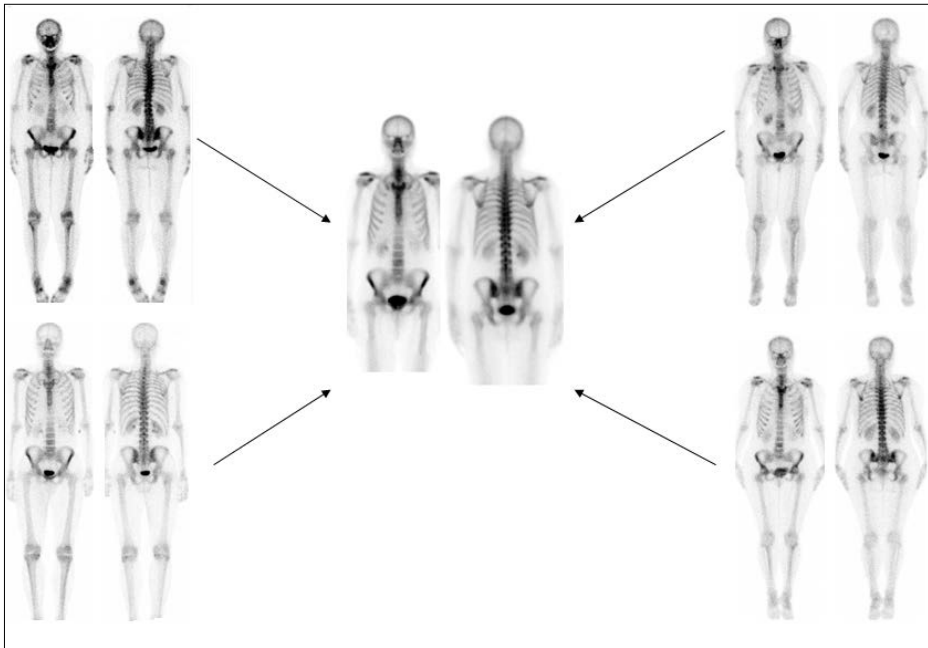


Figure 10. Atlas of normal bone scan, middle, based on 10 normal bone scans from five men and five women, 4 of which showing in the corners.

The manual delineation of the atlas comprises a set of polygons segmenting the skeleton into twelve separate anatomical regions: skull, cervical vertebrae, thoracic vertebrae, lumbar vertebrae, sacrum, pelvis, ribs, scapula, humerus, and femur in both the anterior and the posterior images, and clavicle and sternum in the anterior image. Fig. 11 shows the delineated anterior image of a patient with a normal bone scan acquired using a gamma camera.

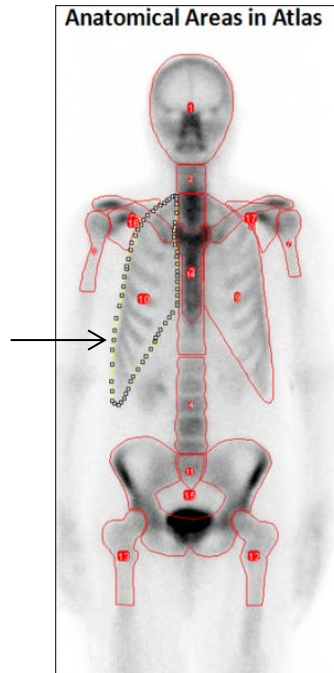


Figure 11. Anatomical area in an anterior bone scan delineated in twelve anatomical regions. Black arrow shows manual drawing of right anterior ribs in the normal atlas.

The transformation between the atlas and a patient skeleton (or between two normal bone scans, as in the atlas-building process described above) is established using a technique of non-rigid image registration (60). This transformation can be used to segment the patient skeleton. Once the transformation from the atlas to the patient skeleton has been acquired, the manual delineation of the atlas image can be transformed accordingly. If the transformed atlas is in full correspondence with the patient skeleton, an accurate segmentation of the patient skeleton is provided.

The registration algorithm is a slightly modified version of the Morphon method (60, 61). The aim of the modification is to increase robustness for the purpose of segmenting skeletal images, both anterior and posterior images being supplied. The Morphon registration method proceeds in iterations, with each iteration bringing the atlas image into closer correspondence with the patient image. The algorithm is first run on sub-sampled and blurred versions

of the images in order to avoid erroneous matching with small-scale image structures. As the atlas image is brought into closer correspondence with the patient skeleton, increasingly higher-resolution images are considered until the registration converges.

3.3 Normalisation and hotspot detection

The segmentation provides the necessary anatomical information for accurately normalising the image to a reference average count and for segmenting hotspots. The average pixel counts in a selected number of regions of the delineated skeleton are first calculated, and are set to a reference level. Hotspots in the resulting normalised image are then detected and segmented using the technique described below. The average counts are then once again adjusted, this time considering pixels inside the same skeletal regions but excluding the segmented hotspots. Hotspots are then once again detected and segmented, and average counts are re-evaluated and adjusted. This process is repeated until attainment of convergence, which will be after three or four iterations. Hotspots are segmented using a combination of filtering and thresholding. The skeletal image is first filtered using a difference-of-Gaussians band-pass filter, which emphasises coherent regions of locally elevated counts. The filtered image is then thresholded at a constant level. The resultant segmented regions are accepted as hotspots if they exceed a minimum size and are located inside the skeleton (Fig. 12).

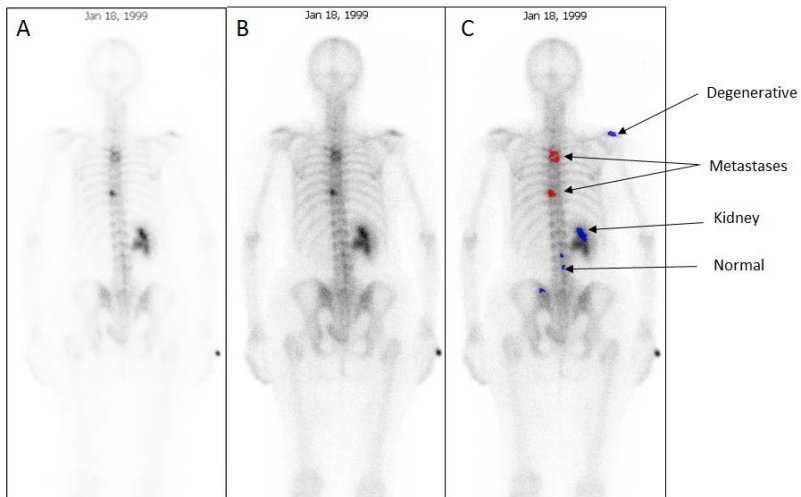


Figure 12. Illustration of a posterior bone scan image before (A,) and after (B), normalization following by hotspots detection(C).

3.4 Hotspot quantification

One of the principal measurements calculated for each hotspot is skeletal involvement. This is defined as the weight of the hotspot with respect to the weight of the entire skeleton (55). This requires estimation of the hotspot volume from one or two two-dimensional projections of the skeletal region that is visible as a hotspot in the images. Obviously this estimation cannot be precise, and we must settle for an estimate that is not significantly and/or systematically different from the true hotspot volume. Estimation of skeletal involvement is based on two measurements and a fixed constant. Firstly, the absolute image area of the hotspot is calculated. The image area of the corresponding skeletal region obtained from the segmentation of the skeleton (e.g. the skull) is then calculated. Dividing the former by the latter provides an estimate of the volumetric fraction of the skeletal region occupied by the hotspot. This value is then multiplied by a constant representing the weight fraction of the present skeletal region with respect to the weight of the total skeleton. These constants – one for each skeletal region – have been estimated from post-mortem studies of bone weight (56). The resulting estimate of skeletal involvement is presented as a percentage of the total skeleton.

The skeletal involvement and a host of other measurements (features) are calculated for each hotspot and are used to classify the hotspots as representing a high or low risk of metastasis. These features describe the geometry, localisation and intensity distribution. The anatomical localisation is described with respect to the skeletal region to which the hotspot belongs, and describes its inferior/superior and medial/lateral position with respect to an accurately determined midline. For some skeletal regions, e.g. the clavicles, features indicate the presence of a hotspot in the contralateral skeletal region that is similar to the current hotspot. In such regions this is indicative of conditions such as arthritis, rather than of metastatic disease. Features are also calculated pertaining to the regional and global density of hotspots, indicating the increased possibility of metastatic disease for a particular hotspot, given a high frequency of hotspots in the rest of the skeleton.

3.5 Hotspot classification

The feature values calculated for each hotspot can be used to determine a value related to the probability of the hotspot being a metastasis. This value can in turn be used to allocate the hotspot to one of two classes – high or low risk of metastasis. Artificial neural networks (ANNs) were used to estimate these probabilities. A general presentation of the ANN technique can be found in the work of Cross et al (62). ANN is a statistical learning method based on examples with a known outcome. A total of 44,570 hotspots were used for training.

A total of 10,826 hotspots were classified as representing a high probability of metastasis, 32,802 as representing a low probability and 942 as representing bladder uptake. Hotspots classified as bladder uptake were automatically excluded from ANN training, since such hotspots can be identified from elementary rules based on localisation and geometry. A total of 12 ANNs were used for training, each corresponding to a skeletal region. This is beneficial, as the appearance of hotspots differs with anatomical localisation. Finally, cut values stratifying the output values according to high or low metastatic probability were chosen for each ANN. The cut values were selected manually based on the false positive/negative rates obtained in the training group (Fig. 11).

After a whole-body bone scan has been acquired using a gamma camera, the anterior and posterior images can be processed using quantification software (Exini bone), and in a few seconds hotspots will be marked in red if they have been classified as pathological lesions and in blue if have been classified by the automated software as being non-metastatic (Fig. 13).



Figure 13. Routine bone scan images (anterior and posterior projections) before (left) and after (right) hotspots detection and classification. Red marks demonstrate hotspots with high-risk probability of metastases. Blue marks indicating hotspots with low-risk probability of metastases.

3.6 Bone Scan Index

Visual inspection, counting the number of metastases from 0 to >20 and a superscan (widely metastasised bone scan) constituted a quantification method for visualising the extent of skeletal disease showed by Soloway et al (63). Calculation of Bone Scan Index (BSI) was presented by a group from Memorial Sloan-Kettering Cancer Center in the late 90s (55). Erdi et al demonstrated that the extent of metastatic lesions in bone is an indicator of prediction of survival in patients with metastatic PCa. They presented a semi-automated method for calculation of BSI, and showed why the important part of the procedure, i.e. detection of metastatic hotspots, should be carried out by an experienced physician, after which the software can delineate the hotspots and calculate the mass of the total pathological skeletal lesions in the images. Sabbatini et al calculated BSI by scoring each bone scan and using the weight of 158 bones from a reference table (57). This quantification method was not widely accepted by nuclear-medicine physicians, because the calculations involved in each examination were so time-consuming.

Automatic classification of hotspots makes it possible to gather information that is limited to hotspots classified as representing a high probability of metastatic disease. The sum of the skeletal involvement of all high-probability hotspots in the entire skeleton is defined as the BSI. This measure is indicative of the total metastatic burden, and can be reported as being a percentage of the total skeletal weight (55). Fig. 14 demonstrates calculation of BSI in a prostate-cancer patient with metastases in the vertebrae.

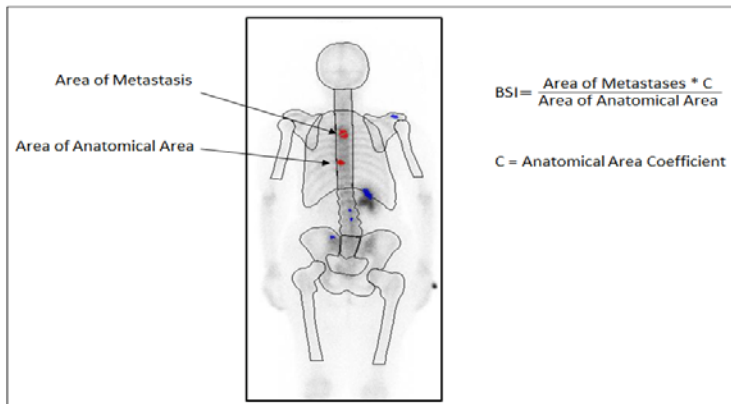


Figure 14. Calculation of BSI in a segmented image of a prostate cancer patient with metastases in vertebrae.

3.7 Bone scan examinations

Bone scans from patients at Sahlgrenska University Hospital, Sweden and Skåne University Hospital, Sweden were obtained between three and four hours after intravenous injection of 600 MBq 99m-technetium MDP (Amersham, UK). Whole body bone scans and anterior and posterior views (scan speed 10 cm/min [training group in Paper I, Paper II, and evaluation group in Paper III] or 15 cm/min [evaluation group in Paper I and treatment group in Paper III], matrix 256 x 1024) were obtained using a gamma camera equipped with low-energy, high-resolution parallel-hole collimators (Maxxus, GE Healthcare, Milwaukee, WI, USA [training group in Paper I, evaluation group in Paper II and evaluation group in Paper III] or MultiSPECT2, Siemens Healthcare Diagnostics, Deerfield, IL, USA [evaluation group in Paper I and treatment group in Paper III]). Energy discrimination was adjusted by a 15% window centred on the 140 keV of Tc 99m (Fig. 15).

Several centres in the United States, Sweden and Canada contributed bone scans for Paper IV. Bone-scan examinations in Paper I and Paper II were obtained less than three months after the diagnosis. In Paper III and Paper IV bone scans were obtained at baseline and during treatment.



Figure 15. Bone scan examination of a PCa patient with a dual detector gamma camera three hours after injection of ^{99m}Tc -MDP.

4 PATIENTS

4.1 Study design

All studies in this thesis are retrospective in design, i.e. we look back in patients' medical history and data to investigate the aims mentioned above. A comparison of retrospective studies with prospective studies shows that the former have advantages and, of course, disadvantages (64). One advantage of a retrospective study is that analysis of long-term follow-up, e.g. five-year survival data, can be obtained immediately. A disadvantage is that not all variables are available for all patients. In Paper I, Paper II and Paper III the patients were selected from clinical cases, thus the indications for performing the bone scans are not clear. The patients in Paper IV were part of a randomised Phase 2 clinical trial, and the indication for the bone scans and their timing was thus stricter, as was the inclusion of other biomarkers. Quantitative analysis of the bone scans was not planned from the start, thus the quality of these scans was not sufficient in all patients.

Paper I and Paper II were prognostic studies focusing on the value of BSI at the time of diagnosis. In Paper III and Paper IV we studied BSI and change in BSI as a biomarker to evaluate treatment response.

4.2 Population

In the four papers that make up this thesis a total of 1,691 patients were included (Table 2). The mean age of the total population was 68, ranging from 25 to 97. Most patients came from Sahlgrenska University Hospital in Gothenburg, Sweden and Skåne University Hospital in Malmö, Sweden.

With the exception of part of the training group in Paper I, the patients in all studies were prostate-cancer patients (Table 2). The training group in Paper I comprised a combination of male and female patients with different kinds of malignant disease, though the majority of them were prostate-cancer and breast-cancer patients. The reason for this non-homogeneous patient selection was that our aim was to develop a quantification method that could be applied to bone scans from patients with different types of cancer. The initial studies included in this thesis focus on patients with prostate cancer, but future studies will also evaluate the value of BSI in other patient groups, e.g. breast-cancer patients.

The evaluation group for Paper I comprised PCa patients from two large screening programmes – the Malmö Preventive Medicine Project and the Malmö Diet and Cancer Study. Patients with a digitally stored whole-body bone scan performed less than three months after diagnosis and a PSA value were included. In Paper II we wanted to confirm the results from Paper I, but this time in a more homogeneous group of PCa patients. In Paper I low-, intermediate- and high-risk patients were included, and treatment after diagnosis was not considered in the analysis. In Paper II we only included high-risk patients who received primary hormonal therapy.

The bone scans in the evaluation groups in Paper I and Paper II were obtained close to the date of diagnosis. Contrastingly, the bone scans analysed in Paper III and Paper IV were obtained from patients at an advanced stage of disease – metastatic castration-resistant prostate cancer. This selection of patients in the different papers facilitated the study of the value of BSI at different stages of disease.

The patients enrolled in Paper IV were part of a Phase II, double-blind, placebo-controlled study of tasquinimod. The patients were randomly divided into two groups, with two thirds of them (n=57) being treated with tasquinimod and a third (n=28) receiving placebo. Tasquinimod is a new drug for treatment of mCRPC that has demonstrated improved progression after six months' treatment. This was our first attempt to use BSI as an objective biomarker to show positive effects of a new drug.

Paper	Training(N)	Diagnosis	Validation(N)	Endpoint
1	795	PCa, Brca, Kica, Blca, other	384	Pca death
2	-	PCa	130	OS
3	266	PCa	31	OS
4	-	PCa	85	OS, treatment effect

Table 2. Population characteristic in development of automated method. PCa= Prostate cancer, Brca= Breast cancer, Kica= Kidney cancer, Blca= Bladder cancer.

5 STATISTICAL ANALYSIS

Pearson's correlation coefficient was used to assess the agreement between the manual and the automated methods of calculating BSI.

Cox proportional-hazards regression models were used to evaluate the association between BSI, other biomarkers (PSA, Gleason score, clinical T-stage, treatment, haemoglobin, pain, PSA doubling time) and survival.

The concordance index (C-index) was used to examine the discrimination between different parameters.

Kaplan-Meier estimates of the survival function together with the *Log-rank test* were used to study differences between groups of patients stratified on the basis of their BSI values.

6 RESULTS

6.1 Automated vs. manual method

The correlation between BSI measurements from the original manual method and BSI from the new automated quantification method was high (Paper I). The agreement between the methods was highest for patients with a few metastases, but for patients with widespread bone metastases there were bigger differences (Fig. 16).

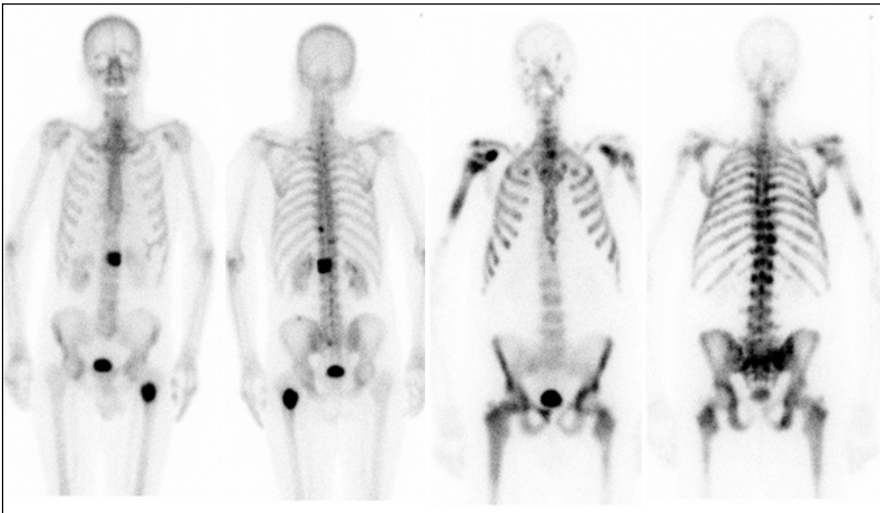


Figure 16. Whole-body bone scan of two PCa patients, one with limited metastatic spread (left) and one with widespread bone metastases(right).

The automated method for detection of new lesions displayed a high degree of sensitivity as well as a high degree of specificity (Paper III), using the interpretations of three experienced readers as the gold standard.

Paper I and Paper III also show the presence of intra-observation and inter-observer variation. In Paper I an experienced reader calculated BSI twice for each bone scan on different occasions, and the results were not identical. In Paper III there was disagreement between the three observers regarding the presence or absence of at least two new lesions in 13% of the cases. These types of disagreement illustrate the value of objective methods featuring a high degree of reproducibility.

The automated method was at least 30 times faster than the manual method at processing and analysing the images and calculating BSI.

6.2 BSI as a prognostic tool

In Paper I survival in patients with a high BSI was significantly inferior to survival in those with a low BSI. Kaplan-Meier curves showed that in patients with a BSI of under 1.0 the prognosis was similar to that for patients without metastases. Adding automated BSI to a base model comprising PSA, Gleason score and T-stage improved the C-index, raising it from 0.768 to 0.825.

In Paper II the 130 high-risk PCa patients had a 41% chance of five-year survival. Those patients with metastases had a 24% chance of five-year survival, whilst the patients without metastases had more than double the chance of still being alive after five years. Stratifying the high-risk PCa patients into subgroups with different levels of BSI at the time of diagnosis showed that those with $BSI > 5$ were all dead after five years, whereas 55% of those with $BSI = 0$ were alive after the same period (Fig. 17). In a multivariate analysis BSI ($p < 0.001$) and Gleason score ($p = 0.01$) were significantly associated with overall survival, whilst PSA ($p = 0.57$) and T-stage ($p = 0.29$) were not.

In Paper IV BSI was correlated with survival in both univariate and multivariate analysis, together with PSA doubling time, tumour pain and treatment arm. A baseline of $BSI < 1.0$ was associated with longer survival than in men with $BSI > 1.0$.

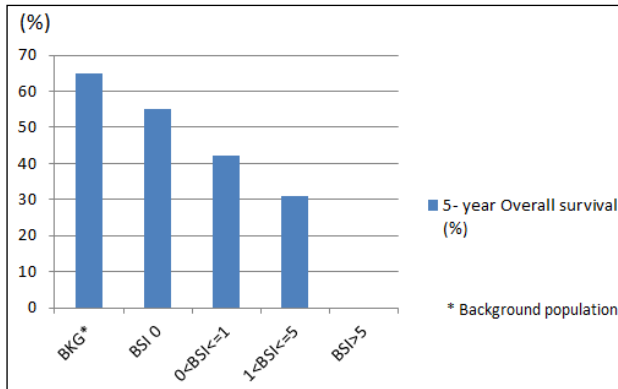


Figure 17. Five-year overall survival for advanced prostate cancer patients with different BSI levels.

6.3 BSI as a treatment- response tool

In Paper III BSI was calculated before and after treatment with chemotherapy in a group of 31 patients with metastatic castration-resistant prostate cancer. A total of 55% of these patients displayed an increase in BSI during treatment, and 82% of them were dead after two years' follow-up. The corresponding level in 45% of patients with a decrease in BSI was a 43% mortality rate after two years' follow-up. Both the percentage change in BSI ($p=0.008$) and the number of new lesions ($p=0.0004$) were associated with survival in univariate analyses.

In Paper IV the relative change in BSI from baseline to 12 weeks after commencement of treatment prognosticated survival in a multivariate analysis including baseline BSI and tasquinimod treatment. The increase in BSI at Week 12 vs baseline was slower with tasquinimod than with placebo (0.16 ± 0.41 vs 0.26 ± 0.49 BSI increase).

7 DISCUSSION

Interpretation of bone scans is a subjective process that is dependent on the experience and knowledge of the nuclear-medicine physician in question. Reports often express a degree of uncertainty, e.g. 'may be degenerative' or 'possible metastasis', and the tumour burden can be expressed as 'extensive metastatic disease' and 'some spread of metastases'. This type of final reporting has the disadvantage that it may be perceived differently by the nuclear-medicine physician and the referring physician. This type of misunderstanding in communications may lead to inappropriate or incorrect treatment in patients with severe disease, and an effective medication may be stopped as a result of a misconception. Quantitative standardisation of the final reports so as to minimise the risk would thus be of value. Trägårdh et al reported that almost half of the referring physicians underestimated the extent of the ischaemic or infarction area in stress myocardial perfusion scintigraphy reported by nuclear-medicine physicians (65).

Manual interpretation of serial bone scans is also subjective. The reporting physician often expresses the intensity or size of the hotspots when assessing the progress of disease after treatment, and this may result in an incorrect conclusion on the part of the referring physician. Counting metastases, as reported by Soloway et al, is one method of quantification (63). The Prostate Cancer Clinical Trials Working Group (PCWG2) defined progression in bone as the presence of two or more new lesions on a bone scan when it is compared with a prior bone examination. They recommended a confirmatory bone scan three to six months later, to minimise the risk of falsely reporting progression, e.g. as a result of a flare phenomenon (66). Expression of disease progress in numerical terms is common in clinical trials, as PCWG2 defines above. Measurement of BSI by the research group at the Memorial Sloan-Kettering Cancer Center in New York was another step towards quantitative reporting (55). Quantitative analysis of bone scans may lead to a clearer message being sent to referring physicians. Our automated method of calculating BSI and detecting new lesions in bone scans in a matter of seconds may be a useful tool both in clinical use and in clinical trials (67, 68).

The results of our studies showed that it is possible to develop a method that can calculate tumour burden automatically, with a minimal need for manual steps on the part of the operator. The reproducibility of a completely automated method is 100%, i.e. if the same digital image is analysed twice the automated BSI will be the same. We also showed that the complex

analysis can be performed in under ten seconds. These features are important for acceptance of a method in a clinical setting, especially as it is being applied to the large group of prostate-cancer patients. The cost of a bone scan is low compared to that of other examination modalities, and it is widely available. An easy-to-use method of quantifying BSI could therefore qualify BSI as an imaging biomarker to be used together with PSA and other biomarkers.

In the development of the automated method we used bone scans obtained during the period 1996 to 2006. During this ten-year period different gamma cameras were used and other parameters underwent changes, but the technical quality of the bone scans remained sufficient for a retrospective analysis of these scans. We consider the fact that the automated method can handle bone scans to be a strength, despite some differences in scintigraphic methodology. It is likely that the method can be used without any problems in hospitals using different imaging procedures, as long as the image quality is sufficient.

Another issue with the use of retrospective materials is that a lack of data such as missing PSA values and missing causes of deaths in Paper I is more common than in prospective studies. On the other hand we could apply our new quantification method to bone scans from patients with up to 15 years of follow-up.

In Paper I we applied the automated method to a patient population for which prostate-cancer-specific mortality was available. In Papers II-IV we used the more common endpoint of overall survival. The different endpoints explain the different survival curves presented in these studies. In Paper I the five-year survival for patients with metastatic disease and $BSI < 1.0$ is much higher than in the other papers.

We studied the clinical value of BSI in prostate-cancer patients, but initial developments were based on a training group that also included other types of diagnosis. Inclusion of patients with kidney and bladder cancer should particularly be noted, since these cancers are often associated with osteolytic metastases. However, the method is designed to handle hot spots due to osteoblastic metastases, not cold spots due to osteolytic metastases. The training group also comprised both male and female patients. It is possible that a gender- and disease-specific training database would have improved the performance of the automated method, but the differences between metastatic and non-metastatic findings are probably more pronounced than differences due to gender and type of cancer.

Our primary goal was to develop a quantification method for analysis of a single bone-scan examination. The automatically calculated BSI proved to be associated with survival in prostate-cancer patients. These results encouraged us to take the method one stage further, and to analyse bone scans from the same patient. This analysis was the most interesting one from a clinical point of view, since treatment response is commonly evaluated using serial bone scans. We developed the method to mimic analysis by an experienced reader. For each lesion detected in the current scan the same anatomical site in the previous scan is scrutinised to assess whether the lesion was present previously or whether it is new. This type of serial analysis is performed both in clinical trials and in routine clinical procedure for the detection of progressive disease. The decision whether or not to continue a treatment depends on the presence or absence of progressive disease. This decision is very important for the patient. The risk of stopping a potentially effective treatment or continuing an ineffective treatment with side effects must be minimised. From a healthcare perspective it is also important that new and expensive treatments only be offered to patients who will benefit from them.

The automated method for detection of new lesions in follow-up scans displayed high levels of sensitivity (93%) and specificity (87%). These results are good, considering that even the experienced bone-scan readers in our study did not always agree. Sadik et al also studied inter-observer variability by having 37 readers interpret the same 59 bone scans (69). They demonstrated agreement of 64% between paired observers while assessing the same bone-scan images, which is a much lower percentage than our result in this paper. The lower level of agreement in the Sadik et al study was probably partly due to the observers in that study being from different hospitals and their use of a four-degree classification scale, whilst the bone-scan readers in our study were all from the same hospital and used a two-degree classification scale.

8 CONCLUSION

The global total of older men with prostate cancer is continuously increasing. New treatment options that can improve survival and quality of life in this patient group will be available in the near future. These new and expensive drugs may increase healthcare costs. We thus need to find new strategies to optimise the treatment of prostate cancer so we get the maximum patient benefit at the minimum cost to the healthcare system.

The results of this thesis indicate that BSI could be a valuable imaging biomarker in the management of prostate-cancer patients. The method of calculating BSI was presented more than 13 years ago, but it has not been widely used. The method was manual and time-consuming, and thus not suitable for clinical use. We developed a fully automated method that can calculate BSI in under ten seconds. We demonstrated a good level of agreement between manual and automated BSI.

In Paper I and Paper II we showed the prognostic value of BSI in prostate-cancer patients at the time of diagnosis. BSI was associated with survival, and may become a prognostic biomarker in addition to the conventional biomarkers used for risk stratification in PCa patients.

In Paper III and IV we showed that BSI and BSI-change on-treatment were associated with survival and may become an imaging biomarker for treatment response analysis in PCa patients.

9 DISCLOSURE

Jens Richter, Karl Sjöstrand, Mattias Ohlsson and Lars Edenbrandt are shareholders in EXINI Diagnostics AB, which provides CAD software for nuclear medicine studies. All other cowriters have nothing to disclose.

ACKNOWLEDGEMENTS

I would like to express my deepest gratitude to my supervisor and mentor Prof. **Lars Edenbrandt**, who gave me the opportunity of studying at Gothenburg University and welcomed me into the research community. His vast knowledge and great wisdom helped me resolve various problems during these years of study. Thank you for inviting me into your academic world and for showing me how to carry out ethical and honest scientific research – I am so grateful for having had the opportunity of working with you.

I also wish to thank my joint supervisor and head of department **Peter Gjertsson**, as well as the senior physician **Milan Lomsky**, who was supportive and encouraging and who helped me assess bone-scan images. I much appreciate their contribution and the friendly discussions I have had with them.

I would further like to express my gratitude to my department – Clinical Physiology and Nuclear Medicine – and to all the staff who helped me carry out my research and made it possible to combine clinical tasks with medical investigation. The combination of clinical work and research tasks would not have been possible if my colleagues from Nuclear Medicine had not been flexible in terms of adjusting the daily schedule, and for this I would particularly like to thank **Carina Höök** and **Maria Sallerup Reid**.

I am most grateful to Prof. **Jan-Erik Damber** from the Department of Urology at Sahlgrenska University Hospital, who helped me better understand issues concerning prostate cancer and its diagnosis and treatment.

I am also grateful for all the statistical assistance I received from Prof. **Mattias Ohlsson**, as well as the technical support provided by **Karl Sjöstrand** and other staff at **Exini Diagnostic AB**.

I am indebted to Dr **Michaela Moonen** for her contribution in terms of constructive discussions and for her scientific review of this work.

My thanks also go to my colleagues from Lund University and Sahlgrenska University Hospital's Department of Radiophysics, to collaborators from the Memorial Sloan-Kettering Cancer Center in New York and to staff from the Nuclear Imaging Group at Sahlgrenska Academy (NIMSA), and special thanks are due to my colleagues Dr **May Sadik** and **Lena Johansson**.

I would furthermore like to express my appreciation of all the **patients** who made this work possible, as well as my respect for them.

I thank all of you who have in any way been involved in the completion of this thesis.

Finally I would like to take this opportunity of thanking **my family**, who were patient and supportive throughout these years.

REFERENCES

1. Jemal A, Bray F, Center MM, Ferlay J, Ward E, Forman D. Global cancer statistics. *CA: a cancer journal for clinicians*. 2011;61(2):69-90.
2. Socialstyrelsen-cancerstatistik. Cancer incidens in Sweden 2011.
3. Nystrand A. Cancer i siffror: populärvetenskapliga fakta om cancer-dess förekomst, bot och dödlighet: Cancerfonden; 2001.
4. Gronberg H. Prostate cancer epidemiology. *The Lancet*. 2003;361(9360):859-64.
5. Carter HB, Epstein JI, Partin AW. Influence of age and prostate-specific antigen on the chance of curable prostate cancer among men with nonpalpable disease. *Urology*. 1999;53(1):126-30.
6. Pienta KJ, Esper PS. Risk factors for prostate cancer. *Annals of internal medicine*. 1993;118(10):793-803.
7. Crawford ED. Epidemiology of prostate cancer. *Urology*. 2003;62(6):3-12.
8. Woolf CM. An investigation of the familial aspects of carcinoma of the prostate. *Cancer*. 1960;13(4):739-44.
9. Bratt O. Hereditary prostate cancer: clinical aspects. *The Journal of urology*. 2002;168(3):906-13.
10. Makridakis NM, Ross RK, Pike MC, Crocitto LE, Kolonel LN, Pearce CL, et al. Association of mis-sense substitution in SRD5A2 gene with prostate cancer in African-American and Hispanic men in Los Angeles, USA. *The Lancet*. 1999;354(9183):975-8.
11. Sofi F, Cesari F, Abbate R, Gensini GF, Casini A. Adherence to Mediterranean diet and health status: meta-analysis. *BMJ: British Medical Journal*. 2008;337.
12. Snowdon DA, PHILLIPS RL, CHOI W. Diet, obesity, and risk of fatal prostate cancer. *American journal of epidemiology*. 1984;120(2):244-50.
13. Hansen A. Nya rön kring omega-3-fettsyror och mental påverkan. 2007.
14. Hiatt RA, Armstrong MMA, Klatsky MAL, Sidney S. Alcohol consumption, smoking, and other risk factors and prostate cancer in a large health plan cohort in California (United States). *Cancer Causes & Control*. 1994;5(1):66-72.
15. Cerhan JR, Torner JC, Lynch CF, Rubenstein LM, Lemke JH, Cohen MB, et al. Association of smoking, body mass, and physical activity with risk of prostate cancer in the Iowa 65+ Rural Health Study (United States). *Cancer Causes & Control*. 1997;8(2):229-38.
16. European Association of Urology, Pocket Guidelines, 2012.
17. Dalton DL. Elevated serum prostate-specific antigen due to acute bacterial prostatitis. *Urology*. 1989;33(6):465.

18. Oesterling JE. Prostate specific antigen: a critical assessment of the most useful tumor marker for adenocarcinoma of the prostate. *The Journal of urology*. 1991;145(5):907-23.
19. Steyerberg E, Roobol M, Kattan M, Van Der Kwast T, De Koning H, Schröder F. Prediction of indolent prostate cancer: validation and updating of a prognostic nomogram. *The Journal of urology*. 2007;177(1):107-12.
20. Moyer VA. Screening for prostate cancer: US Preventive Services Task Force recommendation statement. *Annals of internal medicine*. 2012;157(2):120-34.
21. Heidenreich A, Aus G, Bolla M, Joniau S, Matveev VB, Schmid HP, et al. EAU guidelines on prostate cancer. *European urology*. 2008;53(1):68-80.
22. Hugosson J, Carlsson S, Aus G, Bergdahl S, Khatami A, Lodding P, et al. Mortality results from the Göteborg randomised population-based prostate-cancer screening trial. *The lancet oncology*. 2010;11(8):725-32.
23. Edge SB, Compton CC. The American Joint Committee on Cancer: the 7th edition of the AJCC cancer staging manual and the future of TNM. *Ann Surg Oncol*. 2010;17(6):1471-4. Epub 2010/02/25.
24. D'Amico AV. Biochemical Outcome After Radical Prostatectomy, External Beam Radiation Therapy, or Interstitial Radiation Therapy for Clinically Localized Prostate Cancer. *JAMA: The Journal of the American Medical Association*. 1998;280(11):969-74.
25. Boyle P, Ferlay J. Cancer incidence and mortality in Europe, 2004. *Annals of oncology*. 2005;16(3):481-8.
26. Pili R, Haggman M, Stadler WM, Gingrich JR, Assikis VJ, Bjork A, et al. Phase II randomized, double-blind, placebo-controlled study of tasquinimod in men with minimally symptomatic metastatic castrate-resistant prostate cancer. *Journal of clinical oncology : official journal of the American Society of Clinical Oncology*. 2011;29(30):4022-8. Epub 2011/09/21.
27. Petrylak DP, Tangen CM, Hussain MH, Lara Jr PN, Jones JA, Taplin ME, et al. Docetaxel and estramustine compared with mitoxantrone and prednisone for advanced refractory prostate cancer. *New England journal of medicine*. 2004;351(15):1513-20.
28. Heidenreich A, Schrader AJ. The treatment of hormone refractory prostate cancer. *EAU Update series*. 2003;1(1):40-50.
29. Pili R, Häggman M, Stadler WM, Gingrich JR, Assikis VJ, Björk A, et al. Phase II randomized, double-blind, placebo-controlled study of tasquinimod in men with minimally symptomatic metastatic castrate-resistant prostate cancer. *Journal of Clinical Oncology*. 2011;29(30):4022-8.

30. Ryan CJ, Smith MR, de Bono JS, Molina A, Logothetis CJ, de Souza P, et al. Abiraterone in metastatic prostate cancer without previous chemotherapy. *New England journal of medicine*. 2013;368(2):138-48.
31. Higano CS, Crawford ED, editors. *New and emerging agents for the treatment of castration-resistant prostate cancer*. *Urologic Oncology: Seminars and Original Investigations*; 2011: Elsevier.
32. Bach PB. Limits on Medicare's ability to control rising spending on cancer drugs. *New England journal of medicine*. 2009;360(6):626-33.
33. Engelbrecht MR, Jager GJ, Laheij RJ, Verbeek AL, van Lier H, Barentsz JO. Local staging of prostate cancer using magnetic resonance imaging: a meta-analysis. *European radiology*. 2002;12(9):2294-302.
34. Jacobs SC. Spread of prostatic cancer to bone. *Urology*. 1983;21(4):337.
35. Wang T, Fawwaz RA, Johnson LJ, Mojdehi GE, Johnson PM. Bone-seeking properties of Tc-99m carbonyl diphosphonic acid, dihydroxy-methylene diphosphonic acid and monohydroxy-methylene phosphonic acid: concise communication. *Journal of nuclear medicine: official publication, Society of Nuclear Medicine*. 1980;21(8):767.
36. Peller P, Ho VB, Kransdorf M. Extrasosseous Tc-99m MDP uptake: a pathophysiologic approach. *Radiographics*. 1993;13(4):715-34.
37. Bombardieri E, Aktolun C, Baum RP, Bishof-Delaloye A, Buscombe J, Chatal JF, et al. ¹³¹I/¹²³I-metaiodobenzylguanidine (MIBG) scintigraphy: procedure guidelines for tumour imaging. *European journal of nuclear medicine and molecular imaging*. 2003;30(12):B132-B9.
38. Littlefield JL, Rudd TG. Tc-99m hydroxymethylene diphosphonate and Tc-99m methylene diphosphonate: biological and clinical comparison: concise communication. *Journal of nuclear medicine: official publication, Society of Nuclear Medicine*. 1983;24(6):463.
39. Sadik M, Suurkula M, Hoglund P, Jarund A, Edenbrandt L. Quality of planar whole-body bone scan interpretations--a nationwide survey. *Eur J Nucl Med Mol Imaging*. 2008;35(8):1464-72. Epub 2008/04/01.
40. Hasegawa BH, Wong KH, Iwata K, Barber WC, Hwang AB, Sakdinawat AE, et al. Dual-modality imaging of cancer with SPECT/CT. *Technology in Cancer Research and Treatment*. 2002;1(6):449-58.
41. Rifkin MD, Zerhouni EA, Gatsonis CA, Quint LE, Paushter DM, Epstein JI, et al. Comparison of magnetic resonance imaging and ultrasonography in staging early prostate cancer: results of a multi-institutional cooperative trial. *New England journal of medicine*. 1990;323(10):621-6.
42. Even-Sapir E, Metser U, Mishani E, Lievshitz G, Lerman H, Leibovitch I. The detection of bone metastases in patients with high-

- risk prostate cancer: 99mTc-MDP Planar bone scintigraphy, single-and multi-field-of-view SPECT, 18F-fluoride PET, and 18F-fluoride PET/CT. *Journal of Nuclear Medicine*. 2006;47(2):287-97.
43. SEEMANN MD. Whole-body PET/MRI: the future in oncological imaging. *Technology in cancer research & treatment*. 2005;4(5):577-82.
 44. Cai W, Chen X. Multimodality molecular imaging of tumor angiogenesis. *Journal of Nuclear Medicine*. 2008;49(Suppl 2):113S-28S.
 45. Chenevert TL, Skovoroda AR, Emelianov SY. Elasticity reconstructive imaging by means of stimulated echo MRI. *Magnetic resonance in medicine*. 1998;39(3):482-90.
 46. van den Hoff J, Burchert W, Börner A-R, Fricke H, Kühnel G, Meyer GJ, et al. [1-11C] Acetate as a quantitative perfusion tracer in myocardial PET. *Journal of Nuclear Medicine*. 2001;42(8):1174-82.
 47. Faber TL, Cooke CD, Folks RD, Vansant JP, Nichols KJ, DePuey EG, et al. Left ventricular function and perfusion from gated SPECT perfusion images: an integrated method. *Journal of nuclear medicine: official publication, Society of Nuclear Medicine*. 1999;40(4):650-9.
 48. Boyd N, Byng J, Jong R, Fishell E, Little L, Miller A, et al. Quantitative classification of mammographic densities and breast cancer risk: results from the Canadian National Breast Screening Study. *Journal of the National Cancer Institute*. 1995;87(9):670-5.
 49. Ursin G, Qureshi SA. Mammographic density-a useful biomarker for breast cancer risk in epidemiologic studies. *Norsk epidemiologi*. 2009;19(1).
 50. Germano G, Kiat H, Kavanagh PB, Moriel M, Mazzanti M, Su H-T, et al. Automatic quantification of ejection fraction from gated myocardial perfusion SPECT. *Journal of Nuclear Medicine*. 1995;36(11):2138.
 51. Wolak A, Slomka PJ, Fish MB, Lorenzo S, Acampa W, Berman DS, et al. Quantitative myocardial-perfusion SPECT: comparison of three state-of-the-art software packages. *Journal of nuclear cardiology*. 2008;15(1):27-34.
 52. Spinelli L, Petretta M, Acampa W, He W, Petretta A, Bonaduce D, et al. Prognostic value of combined assessment of regional left ventricular function and myocardial perfusion by dobutamine and rest gated SPECT in patients with uncomplicated acute myocardial infarction. *Journal of Nuclear Medicine*. 2003;44(7):1023-9.
 53. Navare SM, Katten D, Johnson LL, Mather JF, Fowler MS, Ahlberg AW, et al. Risk Stratification With Electrocardiographic-Gated Dobutamine Stress Technetium-99m Sestamibi Single-Photon Emission Tomographic Imaging Value of Heart Rate Response and Assessment of Left Ventricular Function. *Journal of the American College of Cardiology*. 2006;47(4):781-8.

54. Sullivan DC. Imaging as a Quantitative Science. *Radiology*. 2008;248(2):328-32.
55. Erdi YE, Humm JL, Imbriaco M, Yeung H, Larson SM. Quantitative bone metastases analysis based on image segmentation. *The Journal of nuclear medicine*. 1997;38(9):1401-6.
56. Snyder WS, Cook M, Nasset E, Karhausen L, Howells GP, Tipton I. Report of the task group on reference man: Pergamon Oxford; 1975.
57. Sabbatini P, Larson S, Kremer A, Zhang Z-F, Sun M, Yeung H, et al. Prognostic significance of extent of disease in bone in patients with androgen-independent prostate cancer. *Journal of Clinical Oncology*. 1999;17(3):948-.
58. Sadik M, Hamadeh I, Nordblom P, Suurkula M, Höglund P, Ohlsson M, et al. Computer-assisted interpretation of planar whole-body bone scans. *Journal of Nuclear Medicine*. 2008;49(12):1958-65.
59. Guimond A, Meunier J, Thirion J-P. Average brain models: A convergence study. *Computer vision and image understanding*. 2000;77(2):192-210.
60. Wrangsjö A, Pettersson J, Knutsson H. Non-rigid registration using morphons. *Image Analysis: Springer*; 2005. p. 501-10.
61. Knutsson H, Andersson M, editors. Morphons: Segmentation using elastic canvas and paint on priors. *Image Processing, 2005 ICIP 2005 IEEE International Conference on*; 2005: IEEE.
62. Cross SS, Harrison RF, Kennedy RL. Introduction to neural networks. *The Lancet*. 1995;346(8982):1075-9.
63. Soloway MS, Hardeman SW, Hickey D, Todd B, Soloway S, Raymond J, et al. Stratification of patients with metastatic prostate cancer based on extent of disease on initial bone scan. *Cancer*. 1988;61(1):195-202.
64. Doll R. Cohort studies: history of the method II. Retrospective cohort studies. *Sozial-und Präventivmedizin*. 2001;46(3):152-60.
65. Trägårdh E, Höglund P, Ohlsson M, Wieloch M, Edenbrandt L. Referring physicians underestimate the extent of abnormalities in final reports from myocardial perfusion imaging. *EJNMMI research*. 2012;2(1):1-8.
66. Scher HI, Halabi S, Tannock I, Morris M, Sternberg CN, Carducci MA, et al. Design and end points of clinical trials for patients with progressive prostate cancer and castrate levels of testosterone: recommendations of the Prostate Cancer Clinical Trials Working Group. *Journal of Clinical Oncology*. 2008;26(7):1148-59.
67. Ulmert D, Kaboteh R, Fox JJ, Savage C, Evans MJ, Lilja H, et al. A novel automated platform for quantifying the extent of skeletal tumour involvement in prostate cancer patients using the Bone Scan Index. *European urology*. 2012;62(1):78-84. Epub 2012/02/07.
68. Kaboteh R, Gjertsson P, Leek H, Lomsky M, Ohlsson M, Sjöstrand K, et al. Progression of bone metastases in patients with prostate cancer-

- automated detection of new lesions and calculation of bone scan index. *EJNMMI research*. 2013;3(1):1-6.
69. Sadik M, Suurkula M, Höglund P, Järund A, Edenbrandt L. Quality of planar whole-body bone scan interpretations—a nationwide survey. *European journal of nuclear medicine and molecular imaging*. 2008;35(8):1464-72.

ORIGINAL PAPERS